

Synthesis and fabrication of superstrate and substrate $\text{Cu}_2\text{ZnSnS}_4/\text{CdS}$ thin film solar cells utilizing copper powder as local materials

Eka Cahya Prima, Anggi Datiatur Rahmat, and Andhy Setiawan

Solar Energy Materials Laboratory, Universitas Pendidikan Indonesia, Bandung, Indonesia

Email: ekacahyaprima@upi.edu

Abstract

$\text{Cu}_2\text{ZnSnS}_4$ is a promising material for low-cost thin-film solar cells. This paper reports a new approach to fabricating a solar cell using a Superstrate and Substrate configuration. We utilized a non-vacuum deposition process to deposit Copper Zinc Tin Sulfate (CZTS) and Cadmium Sulphate (CdS) on a glass substrate. To achieve this, we adopted the sol-gel spin coating method for CZTS and the Chemical Bath Deposition (CBD) method for the CdS layer. The solar cell has two structures: ITO/ $\text{Cu}_2\text{ZnSnS}_4/\text{CdS}/\text{Ag}$ for substrate configuration and ITO/ $\text{CdS}/\text{Cu}_2\text{ZnSnS}_4/\text{Ag}$ for superstrate configuration. The Cu/(Zn+Sn) atomic ratio was set to 0.86, while Zn/Sn was set to 1.25. Our CZTS/CdS solar cell achieved a 48.7×10^{-6} % power conversion efficiency with a 1.40 eV band gap and 98.71 % external quantum efficiency at 373 nm for the superstrate configuration. For the substrate configuration, the power conversion efficiency was 19.0×10^{-6} % with a 1.49 eV bandgap and 95.74 % external quantum efficiency at 321 nm. Based on the results presented in the text, the CZTS solar cell with a superstrate configuration achieved a higher power conversion efficiency and external quantum efficiency than the substrate configuration. The superstrate configuration allowed for better light absorption in the CZTS layer and reduced the reflection of light back into the substrate. This configuration also prevented the back diffusion of CdS into CZTS and improved the electrical performance of the solar cell. Therefore, the superstrate configuration is more efficient than the substrate configuration for CZTS solar cells.

Keywords: Solar cells, Thin film, $\text{Cu}_2\text{ZnSnS}_4$, Semiconductor, Solution process

Received October 4, 2022, Revision April 24, 2023,
Accepted for publication on April 27, 2023.

<https://doi.org/10.12928/jrkpf.v10i1.234>

This is an open-access article under the [CC-BY-NC](https://creativecommons.org/licenses/by-nc/4.0/) license.



I. Introduction

The issue of energy has become a critical topic in human civilization as the demand for energy continues to increase, particularly the use of electrical energy for daily activities [1], [2]. With the global population constantly increasing, and massive industrialization contributing to environmental pollution, it is becoming increasingly evident that humans need to adopt green energy policies. This is not only to provide a sustainable solution to the increasing demand for energy but also to mitigate the negative impacts of industrialization on the environment. Therefore, there is a need to shift towards the use of clean and renewable energy sources that are sustainable and have a minimal impact on the environment. This shift will require significant changes in the way we generate, distribute and consume energy. Governments, industries, and individuals must work together to adopt green energy policies and technologies that promote the use of renewable energy sources, such as solar, wind, and hydroelectric power, to ensure a sustainable future for the planet [3], [4].

Solar energy is an excellent alternative renewable energy source in the future to replace fossil fuels [1], [5]–[9]. This statement is that solar cells do not produce environmental pollution and can fulfill energy needs

because of their abundant materials [10]–[13]. Various studies have been conducted in recent years to reduce the cost of manufacturing solar cell systems [14], [15]. The cost of producing solar cells also needs to be reduced significantly to produce cheap solar cells with good performance so they can compete in the market to enter the multi-terawatt era (TWatt). Solar cell efficiency is essential for minimizing production costs [16]–[18].

Solar cells have evolved over the years, and significant advancements have been made to improve their efficiency and reduce their cost [19]. The first-generation solar cells, which were made of crystalline silicon, dominated the market for several years [20]. However, their high cost and low efficiency led to the development of second-generation solar cells, which used thin-film materials like Cadmium Telluride and Copper Indium Gallium Selenide [21]. These cells were cheaper to produce and had higher efficiencies than first-generation cells.

More recently, third-generation solar cells have been developed, which aim to overcome the limitations of previous generations. These cells use new materials and technologies, such as dye-sensitized solar cells [22], organic solar cells [23], kesterite solar cells [5], [24] and perovskite solar cells [25], which have the potential to achieve higher efficiencies and lower costs.

The development of these new materials and technologies is crucial for the continued growth of the solar industry, as they offer the potential for higher efficiency and lower costs, making solar energy more accessible to a wider range of people [1], [26], [27]. Additionally, the use of these new materials and technologies is more environmentally friendly, as they require fewer resources to produce, and have a lower environmental impact. As such, the continued development of first, second, and third-generation solar cells is important for the growth of the solar industry and the transition to a more sustainable future. Consequently, the third generation emerging solar cell was now investigated by several researchers around the world to attain a qualified solar cell with high material availability.

In recent years. Kesterite solar cells are a type of thin-film solar cell that has gained significant attention due to their potential for high efficiency, low cost, and the use of earth-abundant materials [28]–[31]. The kesterite structure consists of a tetrahedral network of Cu, Zn, Sn, and chalcogenide (Se, S) ions [15], [32], [33]. The unique feature of the kesterite structure is that it has a high degree of structural flexibility, which enables the substitution of different elements in the structure without altering its properties. This makes it possible to optimize the composition of the kesterite material to improve its efficiency.

One of the main advantages of kesterite solar cells is their potential for high efficiency. Currently, the record efficiency for CZTS kesterite solar cells is 12.6%, which is comparable to the efficiency of second-generation thin-film solar cells [34]. Additionally, kesterite solar cells have the potential to be produced at low cost, since they can be fabricated using non-vacuum methods, such as solution-based techniques like chemical bath deposition or spray pyrolysis. Another advantage of kesterite solar cells is that they are made of abundant elements, which makes them more sustainable and environmentally friendly than other solar cell technologies. The use of abundant elements also reduces the reliance on rare and expensive materials, such as those used in first-generation solar cells.

Despite their potential advantages, kesterite solar cells still face some challenges that need to be addressed, such as improving their stability and increasing their efficiency. However, the continued research and development of kesterite solar cells is expected to result in improved performance and lower costs, making them a promising candidate for future photovoltaic technology [34].

Copper zinc tin sulfide (CZTS) solar cells are a type of thin-film solar cell that is based on abundant and environmentally friendly materials, making them a promising candidate for low-cost and sustainable photovoltaic technology. There are two types of CZTS solar cell structures: substrate configuration and superstrate configuration [35], [36].

In the substrate configuration, the solar cell structure is built on a substrate material such as glass or metal foil. The layers of the solar cell are deposited sequentially onto the substrate in a specific order to form the final structure. In CZTS solar cells, the substrate configuration typically consists of a layer of transparent conductive oxide (TCO) on top of the substrate, followed by a layer of CZTS as the absorber layer, a layer of cadmium sulfide (CdS) as the buffer layer, and a layer of metal (e.g. silver) as the back contact [35], [36].

In the superstrate configuration, the solar cell structure is built on a transparent material such as glass. The layers of the solar cell are deposited sequentially onto the transparent material in a specific order to form the final structure. In CZTS solar cells, the superstrate configuration typically consists of a layer of TCO on the bottom, followed by a layer of CdS as the buffer layer, a layer of CZTS as the absorber layer, and a layer of metal (e.g. silver) as the back contact [35], [36].

The superstrate configuration offers several advantages over the substrate configuration. Firstly, since the TCO layer is on the bottom, it provides a smooth and uniform surface for the deposition of subsequent layers, which can improve the overall performance of the solar cell. Secondly, since the superstrate configuration is built on a transparent material, it allows more light to enter the absorber layer, which can increase the overall efficiency of the solar cell. Lastly, the superstrate configuration allows for easier encapsulation of the solar cell, which can improve its durability and stability. Furthermore, the substrate configuration also has some advantages over the superstrate configuration. One advantage is that it is less sensitive to moisture and oxygen, which can degrade the performance of the solar cell over time. Additionally, the substrate configuration can be more suitable for flexible and lightweight solar cell applications, since it can be fabricated on flexible substrates such as metal foils [35].

The Shockley and Queisser limit photon-balanced theoretical calculation estimates that the efficiency of CZTS thin-film solar cells can reach about 32.2% [24], [37], [38]. On the other hand, due to their features that allow for the rapid fabrication of tandem devices and the lack of surface encapsulation, the superstrate type solar cells still need to receive more research. [39]. In addition, compared to substrate-type solar cells, this type of solar cell allows the transparent conductive oxide (TCO) contact materials to be easily deposited on a glass substrate without the need for a vacuum-based approach. Although the superstrate arrangement has some advantages, the low annealing treatment is blamed for the absorber materials' poor crystallinity. Inter-diffusion between the n-type buffer and the p-type absorber layers occurs when the annealing temperature is raised to enhance the crystallinity of the absorber. This phenomenon affects the device efficiency adversely [10], [29], [40].

This work will directly compare superstrate and substrate configuration and deposition of CZTS and CdS using the non-vacuum method. We provided two CZTS samples (substrate and superstrate) with the same treatment and different structure configurations. The film used the same solution, and the CZTS substrate type was followed by the same sulfurization process, while the CZTS substrate was without the sulfurization process. Usually, substrate-type solar cells have been used with molybdenum back contact, but we will report the use of ITO glass for comparing both samples and using copper powder (99% purity) as west java local material in this work for the first time.

II. Methods

Film Preparation: The thin films were deposited using the spin-coating process. The spin-coating solution was made by dissolving copper (0.52 mol L^{-1} , 99% purity, obtained from west java raw materials), zinc acetate dihydrate $\text{Zn}(\text{CH}_3\text{COO})_2 \cdot 2\text{H}_2\text{O}$ (0.33 mol L^{-1}), tin chloride dihydrate $\text{SnCl}_2 \cdot 2\text{H}_2\text{O}$ (0.27 mol L^{-1}), and thiourea $\text{CH}_4\text{N}_2\text{S}$ (2.06 mol L^{-1}) in 2-methoxy ethanol at 50°C for 2 h. The solution's nominal Cu/(Zn + Sn) and Zn/Sn ratios are 0.86 and 1.25, respectively. Moreover, a few drops of trimethylamine and monoethyl amine were added to the solution. And then make a buffer layer. The CdS solution was prepared by diluting 0.75 M Thiourea, 0.015 M CdSO_4 , and 0.015 M NH_3 in 40 ml deionized water stirred at 50°C for 15 minutes.

The first spin-coating CZTS was prepared for substrate configuration where ITO glass was placed on the spin coater and turned on spin coater. The CZTS solution was dropped on the surface and spun at 4000 rpm for 30 seconds. The film was afterward placed on a 200°C hotplate surface for 2 minutes and cooled down for 3 minutes. The same spin coating processes were repeated 5 times. Next, the sulfurization was started by placing the sample into a furnace tube. The sulfur powder on the tube's side was set to 550°C for 30 minutes. The process was followed by the chemical bath deposition method at 80°C for 9 minutes to make the $\sim 60 \text{ nm}$ CdS film. The film was then washed using a water air blower and placed in an oven at 50°C for 15 minutes. Finally, the ITO/CZTS/CdS film was prepared as a sample substrate.

Moreover, for the superstrate type, first, make the CdS film by chemical bath deposition with the same treatment at the structure Substrate. Then is followed by spin-coating CZTS. Afterward, annealing film at 550°C for 30 minutes without using sulfur. Finally, the ITO/CdS/CZTS film was prepared as a sample superstrate. After both samples were prepared, the silver paste was used as the top contact. Next, the paste was heated at 50°C for 3 minutes, and the sample was prepared for future analysis.

Characterization: Optical absorption characterization using UV-Vis Spectrometry is aimed at determining the optical characteristics of the CZTS absorber layer. With this characterization, the optical properties (absorbance) and Bandgap Energy (E_g) can be determined.

Electrical characteristics that are tested include the I - V characteristics of the solar cell which are necessary to determine the generated current density (I_{sc}), open-circuit voltage (V_{oc}), efficiency, and fill factor (FF) of

the tested solar cell. The I - V characteristics of the solar cell are necessary to determine the generated current density (I_{sc}), open-circuit voltage (V_{oc}), efficiency, and fill factor (FF) of the tested solar cell. A xenon lamp with a power of 450W was used to measure the current and voltage using the ADCMT DC Voltage/Current Source/Monitor 6242.

To determine the absorption characteristics of the CZTS absorber layer, characterization testing is performed using UV-Vis spectroscopy. The results of the testing are used to determine the energy gap (E_g) and light harvest efficiency (LHE). To determine the effect of absorbance on wavelength, the absorbance is plotted against the wavelength. There is a relationship between LHE and α . The LHE value can be obtained using the absorbance data (α) as shown in Equation (1).

$$LHE(\%) = 1 - 10^{-\alpha} \times 100\% \tag{1}$$

To determine the bandgap energy, the Tauc plot method is used [41], [42]. The Tauc plot method involves drawing a straight line between the product of the absorbance coefficient (α) and the absorbed photon energy ($h\nu$). This results in the bandgap energy value. Here, α is the absorbance, h is Planck's constant, and ν is the frequency obtained by inserting the wavelength data into Equation 2:

$$\nu = c / \lambda \tag{2}$$

The data is then plotted against energy ($h\nu$) to obtain a Tauc plot graph, and the bandgap value is read based on the straight line drawn between $h\nu$ and $(\alpha h\nu)^2$. Next, an analysis is performed and the results of the UV-Vis characterization data are compared by comparing the different Cu concentrations in each sample, in order to determine the effect of Cu concentration on the optical absorption characteristics.

III. Results and discussion

The architectural design and the photograph of the CZTS solar cell are shown in Figure 1. The figure discussed the photograph for substrate and superstrate film.

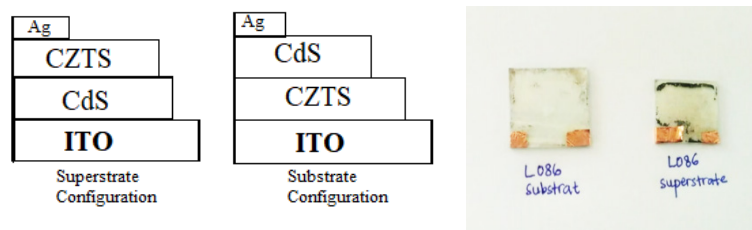


Figure 1. Superstrate and Substrate configurations of a solar cell (left) and the photograph of CZTS solar cells (right)

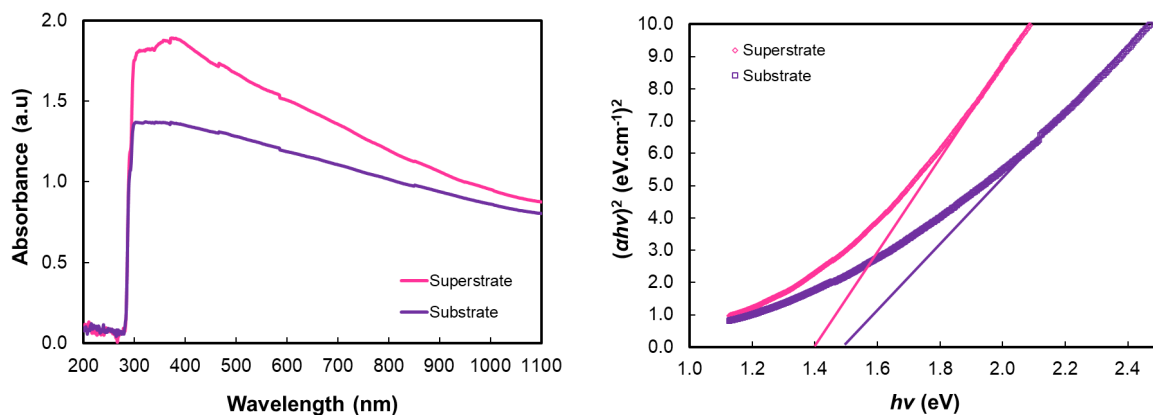


Figure 2. Film absorbance (left), Band gap analysis of Cu_2ZnSnS_4 thin-film solar cells

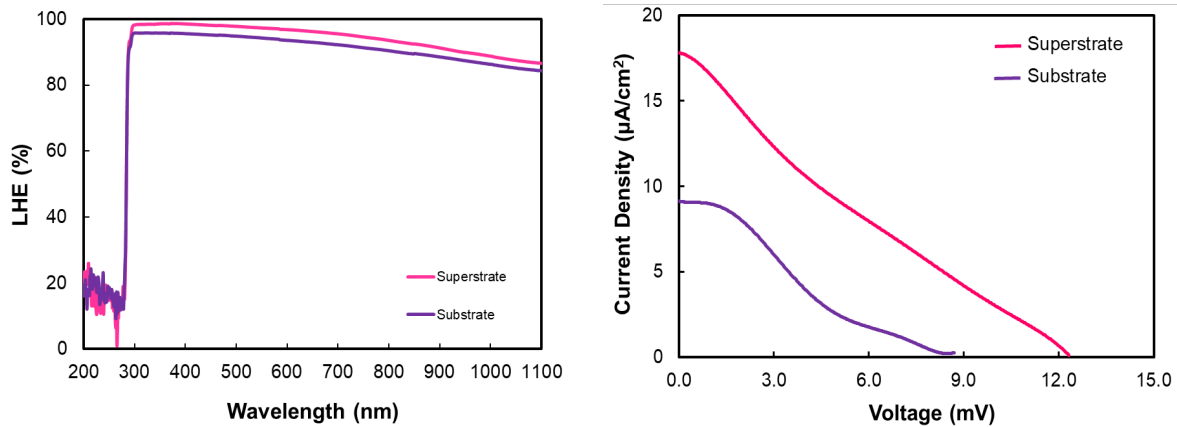


Figure 3. The light-harvesting efficiency of solar cells (left), J - V curves of solar cells (right)

The Optical Bandgap is determined from the Tauc equation [41], [42]:

$$\alpha hv = A(hv - E_g)^n \quad (3)$$

Where α is the absorption coefficient, hv is the energy of the incident photons, $n = \frac{1}{2}, \frac{3}{2}, 2$, and 3 for direct allowed, direct forbidden, indirect allowed, and indirect forbidden transitions, respectively, and A is constant. The absorption coefficient α can be determined by mathematical treatment of the absorbance vs. wavelength spectrum for the wavelength range obtained in Figure 2. Tauc's plots were drawn between photon energy and $(\alpha hv)^2$. The optical band gap is deduced by extrapolating the linear portion of the $(\alpha hv)^2$ vs. hv plot to meet the hv axis where the value of αhv is zero, the intercept of the x -axis gives the Bandgap E_g .

Table 1. The IPCE analysis for the $\text{Cu}_2\text{ZnSnS}_4$ thin-film solar cells

Samples	λ_{max} (nm)	LHE_{max} (%)	E_g (eV)
Superstrate	373	98.71	1.40
Substrate	321	95.74	1.49

Table 1 shows the results of IPCE (incident photon-to-current conversion efficiency) analysis for two types of $\text{Cu}_2\text{ZnSnS}_4$ thin-film solar cells, one with a superstrate configuration and the other with a substrate configuration. The first column lists the samples, while the second column indicates the wavelength (in nanometers) at which the maximum IPCE was achieved. The third column shows the maximum LHE (light harvesting efficiency) in percentage, which indicates the percentage of light energy converted into electrical current. The last column shows the bandgap energy (in electron volts, eV) of the samples, which is the minimum energy required for an electron to move from the valence band to the conduction band and conduct electricity. The data suggests that the superstrate configuration has a higher LHE and a lower bandgap energy compared to the substrate configuration.

Figure 2 presents that the CZTS layer absorbs the wavelength spectrum between 200-1100 nm. As seen in Table 1, the bandgap analyzed from the LHE plot results in 1.40 and 1.49 eV for sample superstrate and substrate, respectively. The narrower superstrate's sample bandgap is due to the absorber layer being better at 0.9% kesterite phase. The incident photon-to-current conversion efficiency also supports the broadening light absorption spectrum for sample superstrate with a higher maximum peak at 570 nm, and the maximum light-harvesting efficiency (LHE) is 98.71%, as also seen in Figure 3.

Light harvesting efficiency (LHE) in Figure 3 measures how effectively the device converts incident light into usable electrical energy. It is calculated as the ratio of the number of photons that are converted into electrical energy to the total number of photons that are incident on the device. The higher the LHE, the more efficient the solar cell is in converting light into electricity. LHE is an important parameter to consider when designing and optimizing solar cells for maximum efficiency and performance.

The power conversion efficiency η of solar cells is calculated using

$$\eta = \frac{J_{sc} V_{oc} FF}{P_{in}} \times 100\% \quad (4)$$

where FF is the fill factor and is determined as:

$$FF = \frac{J_{max} V_{max}}{J_{sc} V_{oc}} \quad (5)$$

Table 2. Photovoltaic performance for the $\text{Cu}_2\text{ZnSnS}_4$ thin-film solar cells

Parameters	J_{sc} ($\mu\text{A.cm}^{-2}$)	V_{oc} (mV)	J_{max} ($\mu\text{A.cm}^{-2}$)	V_{max} (mV)	FF (%)	$\eta \times 10^6$ (%)
Superstrate	17.71	12.32	8.00	6.09	22.3	48.7
Substrate	9.14	8.70	6.29	3.02	23.9	19.0

Table 2 reports J_{max} (maximum current density), V_{max} (maximum voltage), V_{oc} (the open-circuit voltage), J_{sc} (the short circuit current density), and P_{in} (the incident light's power density). The maximum efficiency of $48.7 \times 10^{-6}\%$ with open-circuit voltage V_{oc} 12.32 mV, current density J_{sc} $17.71 \mu\text{A.cm}^{-2}$ and fill factor of 22.3% for CZTS superstrate, and efficiency of $19.0 \times 10^{-6}\%$ with open-circuit voltage V_{oc} 9.14 V, current density J_{sc} $9.14 \mu\text{A.cm}^{-2}$ and fill factor of 23.9% for CZTS substrate. Based on this result, it can be found that solar cells with superstrate configuration have higher efficiency than substrate configuration CZTS solar cells. The higher the film absorbance and the lower the film band gap contribute to improving the cell performance.

Based on Table 2, the limiting factors for the efficiency of the $\text{Cu}_2\text{ZnSnS}_4$ thin-film solar cells are the low short-circuit current density (J_{sc}) and the low fill factor (FF) for both superstrate and substrate samples. The open-circuit voltage (V_{oc}) and maximum power output (P_{max}) are relatively similar for both samples, indicating that the current and fill factor are the main limiting factors for the overall efficiency of the cells. This suggests that improving the charge carrier generation and collection within the cell, as well as reducing the series and shunt resistances, could lead to higher J_{sc} and FF values, resulting in a more efficient solar cell.

IV. Conclusions

We have successfully presented utilizing local materials for $\text{Cu}_2\text{ZnSnS}_4$ thin-film solar cells. Solar cells with superstrate and substrate configuration are obtained by depositing Copper Zinc Tin Sulfate (CZTS) and Cadmium Sulphate (CdS) non-vacuum process. The solar cell fabricated based on $\text{Cu}_2\text{ZnSnS}_4/\text{CdS}$ solution process exhibits the new achievement by utilizing material local of power conversion efficiency of $48.7 \times 10^{-6}\%$ with 1.40 eV bandgap and 98.71% external quantum efficiency at 373 nm for superstrate configuration and power conversion efficiency for substrate configuration $19.0 \times 10^{-6}\%$ with 1.49 eV bandgap and 95.74 % external quantum efficiency at 321 nm. In this work, we find solar cells with superstrate configuration have higher efficiency than substrate configuration CZTS solar cells. This suggests that improving the charge carrier generation and collection within the cell, as well as reducing the series and shunt resistances, could lead to higher J_{sc} and FF values, resulting in a more efficient solar cell.

Acknowledgements

This work was supported by Penelitian Dasar Unggulan Perguruan Tinggi (Grant No. 1250/UN40.LP/PT.01.03/2022), Ministry of Education, Culture, Research, and Technology, Republic of Indonesia 2022.

References

- [1] E. Dogan and F. Seker, "The influence of real output, renewable and non-renewable energy, trade and financial development on carbon emissions in the top renewable energy countries," *Renew. Sustain. Energy Rev.*, vol. 60, pp. 1074–1085, Jul. 2016, doi: [10.1016/j.rser.2016.02.006](https://doi.org/10.1016/j.rser.2016.02.006).
- [2] A. Hobson, "Physics literacy, energy and the environment," *Phys. Educ.*, vol. 38, no. 2, pp. 109–114, Mar. 2003, doi: [10.1088/0031-9120/38/2/301](https://doi.org/10.1088/0031-9120/38/2/301).

- [3] A. R. Pratami, L. S. Riza, and L. Rusyati, "Investigating junior high school students' perception of global warming topic using semantic network analysis," *J. Phys. Conf. Ser.*, vol. 1806, no. 1, p. 012124, Mar. 2021, doi: [10.1088/1742-6596/1806/1/012124](https://doi.org/10.1088/1742-6596/1806/1/012124).
- [4] REN21, "Renewables 2015 Global Status Report," Sep. 2015. [Online]. Available: https://www.ren21.net/wp-content/uploads/2019/05/GSR2015_Full-Report_English.pdf.
- [5] H. S. Nugroho *et al.*, "A progress review on the modification of CZTS(e)-based thin-film solar cells," *J. Ind. Eng. Chem.*, vol. 105, pp. 83–110, Jan. 2022, doi: [10.1016/j.jiec.2021.09.010](https://doi.org/10.1016/j.jiec.2021.09.010).
- [6] E. C. Prima, L. H. Wong, A. Ibrahim, Nugraha, and B. Yulianto, "Solution-processed pure Cu₂ZnSnS₄/CdS thin film solar cell with 7.5% efficiency," *Opt. Mater. (Amst.)*, vol. 114, p. 110947, Apr. 2021, doi: [10.1016/j.optmat.2021.110947](https://doi.org/10.1016/j.optmat.2021.110947).
- [7] R. Inglesi-Lotz and E. Dogan, "The role of renewable versus non-renewable energy to the level of CO₂ emissions a panel analysis of sub-Saharan Africa's Big 10 electricity generators," *Renew. Energy*, vol. 123, pp. 36–43, Aug. 2018, doi: [10.1016/j.renene.2018.02.041](https://doi.org/10.1016/j.renene.2018.02.041).
- [8] M. Ravindiran and C. Praveenkumar, "Status review and the future prospects of CZTS based solar cell – A novel approach on the device structure and material modeling for CZTS based photovoltaic device," *Renew. Sustain. Energy Rev.*, vol. 94, pp. 317–329, Oct. 2018, doi: [10.1016/j.rser.2018.06.008](https://doi.org/10.1016/j.rser.2018.06.008).
- [9] H. Batih and C. Sorapipatana, "Characteristics of urban households' electrical energy consumption in Indonesia and its saving potentials," *Renew. Sustain. Energy Rev.*, vol. 57, pp. 1160–1173, May 2016, doi: [10.1016/j.rser.2015.12.132](https://doi.org/10.1016/j.rser.2015.12.132).
- [10] B. Shin, O. Gunawan, Y. Zhu, N. A. Bojarczuk, S. J. Chey, and S. Guha, "Thin film solar cell with 8.4% power conversion efficiency using an earth-abundant Cu₂ZnSnS₄ absorber," *Prog. Photovoltaics Res. Appl.*, vol. 21, no. 1, pp. 72–76, Jan. 2013, doi: [10.1002/ppp.1174](https://doi.org/10.1002/ppp.1174).
- [11] M. Kumar and C. Persson, "Cu₂ZnSnS₄ and Cu₂ZnSnSe₄ as Potential Earth-Abundant Thin-Film Absorber Materials: A Density Functional Theory Study," *Int. J. Theor. Appl. Sci.*, vol. 5, no. 1, pp. 1–8, 2013, [Online]. Available: [http://www.researchtrend.net/ijtas_2013/1 DR MUKESH.pdf](http://www.researchtrend.net/ijtas_2013/1_DR_MUKESH.pdf).
- [12] D. Han *et al.*, "Deep electron traps and origin of p-type conductivity in the earth-abundant solar-cell material Cu₂ZnSnS₄," *Phys. Rev. B*, vol. 87, no. 15, p. 155206, Apr. 2013, doi: [10.1103/PhysRevB.87.155206](https://doi.org/10.1103/PhysRevB.87.155206).
- [13] T. K. Todorov, K. B. Reuter, and D. B. Mitzi, "High-Efficiency Solar Cell with Earth-Abundant Liquid-Processed Absorber," *Adv. Mater.*, vol. 22, no. 20, pp. E156–E159, May 2010, doi: [10.1002/adma.200904155](https://doi.org/10.1002/adma.200904155).
- [14] A. H. Alami *et al.*, "Low-cost dye-sensitized solar cells with ball-milled tellurium-doped graphene as counter electrodes and a natural sensitizer dye," *Int. J. Energy Res.*, vol. 43, no. 11, pp. 5824–5833, Sep. 2019, doi: [10.1002/er.4684](https://doi.org/10.1002/er.4684).
- [15] W. Li, J. M. R. Tan, S. W. Leow, S. Lie, S. Magdassi, and L. H. Wong, "Recent Progress in Solution-Processed Copper-Chalcogenide Thin-Film Solar Cells," *Energy Technol.*, vol. 6, no. 1, pp. 46–59, Jan. 2018, doi: [10.1002/ente.201700734](https://doi.org/10.1002/ente.201700734).
- [16] S. Abdelhaleem *et al.*, "Tuning the Properties of CZTS Films by Controlling the Process Parameters in Cost-Effective Non-vacuum Technique," *J. Electron. Mater.*, vol. 47, no. 12, pp. 7085–7092, Dec. 2018, doi: [10.1007/s11664-018-6636-4](https://doi.org/10.1007/s11664-018-6636-4).
- [17] Q.-M. Chen, Z.-Q. Li, Y. Ni, S.-Y. Cheng, and X.-M. Dou, "Doctor-bladed Cu₂ZnSnS₄ light absorption layer for low-cost solar cell application," *Chinese Phys. B*, vol. 21, no. 3, p. 038401, Mar. 2012, doi: [10.1088/1674-1056/21/3/038401](https://doi.org/10.1088/1674-1056/21/3/038401).
- [18] B. O'Regan and M. Grätzel, "A low-cost, high-efficiency solar cell based on dye-sensitized colloidal TiO₂ films," *Nature*, vol. 353, no. 6346, pp. 737–740, Oct. 1991, doi: [10.1038/353737a0](https://doi.org/10.1038/353737a0).
- [19] H. Hug, M. Bader, P. Mair, and T. Glatzel, "Biophotovoltaics: Natural pigments in dye-sensitized solar cells," *Appl. Energy*, vol. 115, pp. 216–225, Feb. 2014, doi: [10.1016/j.apenergy.2013.10.055](https://doi.org/10.1016/j.apenergy.2013.10.055).
- [20] D. M. Chapin, C. S. Fuller, and G. L. Pearson, "A New Silicon p-n Junction Photocell for Converting Solar Radiation into Electrical Power," *J. Appl. Phys.*, vol. 25, no. 5, pp. 676–677, May 1954, doi: [10.1063/1.1721711](https://doi.org/10.1063/1.1721711).
- [21] T. Kato, "Cu(In,Ga)(Se,S) 2 solar cell research in Solar Frontier: Progress and current status," *Jpn. J. Appl. Phys.*, vol. 56, no. 4S, p. 04CA02, Apr. 2017, doi: [10.7567/JJAP.56.04CA02](https://doi.org/10.7567/JJAP.56.04CA02).
- [22] E. C. Prima, H. S. Nugroho, Nugraha, G. Refantero, C. Panatarani, and B. Yulianto, "Performance of the dye-sensitized quasi-solid state solar cell with combined anthocyanin-ruthenium photosensitizer," *RSC Adv.*, vol. 10, no. 60, pp. 36873–36886, 2020, doi: [10.1039/D0RA06550A](https://doi.org/10.1039/D0RA06550A).
- [23] C.-R. Zhang *et al.*, "DFT and TD-DFT study on structure and properties of organic dye sensitizer TA-St-CA," *Curr. Appl. Phys.*, vol. 10, no. 1, pp. 77–83, Jan. 2010, doi: [10.1016/j.cap.2009.04.018](https://doi.org/10.1016/j.cap.2009.04.018).
- [24] E. C. Prima *et al.*, "The effect of CuZn+ZnCu defect complex on Cu₂ZnSnS₄ thin film solar cell: A density

- functional theory study,” *Mater. Chem. Phys.*, vol. 296, p. 127192, Feb. 2023, doi: [10.1016/j.matchemphys.2022.127192](https://doi.org/10.1016/j.matchemphys.2022.127192).
- [25] S. Liu *et al.*, “A Review on Additives for Halide Perovskite Solar Cells,” *Adv. Energy Mater.*, vol. 10, no. 13, p. 1902492, Apr. 2020, doi: [10.1002/aenm.201902492](https://doi.org/10.1002/aenm.201902492).
- [26] A. Hidayatno, A. D. Setiawan, I. M. Wikananda Supartha, A. O. Moeis, I. Rahman, and E. Widiono, “Investigating policies on improving household rooftop photovoltaics adoption in Indonesia,” *Renew. Energy*, vol. 156, pp. 731–742, Aug. 2020, doi: [10.1016/j.renene.2020.04.106](https://doi.org/10.1016/j.renene.2020.04.106).
- [27] A. M. Omer, “Sustainable Energy Development, the Role of Renewables and Global Warming,” *J. Sustain. Dev. Stud.*, vol. 1, no. 1, pp. 1–67, 2012, [Online]. Available: <https://infinitypress.info/index.php/jsds/article/viewFile/8/10>.
- [28] Y. Gong *et al.*, “Sn⁴⁺ precursor enables 12.4% efficient kesterite solar cell from DMSO solution with open circuit voltage deficit below 0.30 V,” *Sci. China Mater.*, vol. 64, no. 1, pp. 52–60, Jan. 2021, doi: [10.1007/s40843-020-1408-x](https://doi.org/10.1007/s40843-020-1408-x).
- [29] Z. Su *et al.*, “Device Postannealing Enabling over 12% Efficient Solution-Processed Cu₂ZnSnS₄ Solar Cells with Cd²⁺ Substitution,” *Adv. Mater.*, vol. 32, no. 32, p. 2000121, Aug. 2020, doi: [10.1002/adma.202000121](https://doi.org/10.1002/adma.202000121).
- [30] J. P. Sawant and R. B. Kale, “Surfactant mediated TiO₂ photoanodes and Cu₂ZnSnS₄ counter electrodes for high efficient dye sensitized solar cells,” *Mater. Lett.*, vol. 265, p. 127407, Apr. 2020, doi: [10.1016/j.matlet.2020.127407](https://doi.org/10.1016/j.matlet.2020.127407).
- [31] V. Kumar and V. G. Masih, “Fabrication and Characterization of Screen-Printed Cu₂ZnSnS₄ Films for Photovoltaic Applications,” *J. Electron. Mater.*, vol. 48, no. 4, pp. 2195–2199, Apr. 2019, doi: [10.1007/s11664-019-07053-5](https://doi.org/10.1007/s11664-019-07053-5).
- [32] M. Bercx, N. Sarmadian, R. Saniz, B. Partoens, and D. Lamoen, “First-principles analysis of the spectroscopic limited maximum efficiency of photovoltaic absorber layers for CuAu-like chalcogenides and silicon,” *Phys. Chem. Chem. Phys.*, vol. 18, no. 30, pp. 20542–20549, 2016, doi: [10.1039/C6CP03468C](https://doi.org/10.1039/C6CP03468C).
- [33] N. Sarmadian, R. Saniz, B. Partoens, and D. Lamoen, “First-principles study of the optoelectronic properties and photovoltaic absorber layer efficiency of Cu-based chalcogenides,” *J. Appl. Phys.*, vol. 120, no. 8, p. 085707, Aug. 2016, doi: [10.1063/1.4961562](https://doi.org/10.1063/1.4961562).
- [34] W. Wang *et al.*, “Device Characteristics of CZTSSe Thin-Film Solar Cells with 12.6% Efficiency,” *Adv. Energy Mater.*, vol. 4, no. 7, p. 1301465, May 2014, doi: [10.1002/aenm.201301465](https://doi.org/10.1002/aenm.201301465).
- [35] J. Kaza, M. R. Pasumarthi, and A. P. S., “Superstrate and substrate thin film configuration of CdS/CZTS solar cell fabricated using SILAR method,” *Opt. Laser Technol.*, vol. 131, p. 106413, Nov. 2020, doi: [10.1016/j.optlastec.2020.106413](https://doi.org/10.1016/j.optlastec.2020.106413).
- [36] V. V. Satale and S. V. Bhat, “Superstrate type CZTS solar cell with all solution processed functional layers at low temperature,” *Sol. Energy*, vol. 208, pp. 220–226, Sep. 2020, doi: [10.1016/j.solener.2020.07.055](https://doi.org/10.1016/j.solener.2020.07.055).
- [37] S. Rühle, “Tabulated values of the Shockley–Queisser limit for single junction solar cells,” *Sol. Energy*, vol. 130, pp. 139–147, Jun. 2016, doi: [10.1016/j.solener.2016.02.015](https://doi.org/10.1016/j.solener.2016.02.015).
- [38] W. Shockley and H. J. Queisser, “Detailed Balance Limit of Efficiency of p-n Junction Solar Cells,” *J. Appl. Phys.*, vol. 32, no. 3, pp. 510–519, Mar. 1961, doi: [10.1063/1.1736034](https://doi.org/10.1063/1.1736034).
- [39] J. Gilot, M. M. Wienk, and R. A. J. Janssen, “Measuring the External Quantum Efficiency of Two-Terminal Polymer Tandem Solar Cells,” *Adv. Funct. Mater.*, vol. 20, no. 22, pp. 3904–3911, Nov. 2010, doi: [10.1002/adfm.201001167](https://doi.org/10.1002/adfm.201001167).
- [40] C. Ma *et al.*, “Effect of CZTS/CdS interfaces deposited with sputtering and CBD methods on Voc deficit and efficiency of CZTS solar cells,” *J. Alloys Compd.*, vol. 817, p. 153329, Mar. 2020, doi: [10.1016/j.jallcom.2019.153329](https://doi.org/10.1016/j.jallcom.2019.153329).
- [41] J. Tauc, “Optical properties and electronic structure of amorphous Ge and Si,” *Mater. Res. Bull.*, vol. 3, no. 1, pp. 37–46, Jan. 1968, doi: [10.1016/0025-5408\(68\)90023-8](https://doi.org/10.1016/0025-5408(68)90023-8).
- [42] J. Tauc, R. Grigorovici, and A. Vancu, “Optical Properties and Electronic Structure of Amorphous Germanium,” *Phys. status solidi*, vol. 15, no. 2, pp. 627–637, 1966, doi: [10.1002/pssb.19660150224](https://doi.org/10.1002/pssb.19660150224).